SEMARAK ILMU PUBLISHING

Journal of Advanced Research in Fluid Mechanics and Thermal Sciences

Journal homepage:
https://semarakilmu.com.my/journals/index.php/fluid_mechanics_thermal_sciences/index
ISSN: 2289-7879

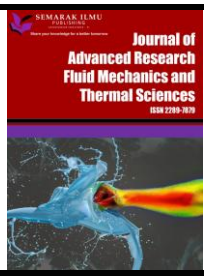

Optimizing Wire Mesh Sensor Design: The Influence of Wire Diameter and Spacing on Bubble Entrapment in Multiphase Flows

Karolina Przybysz[1,2], Dolganov Iurii[1,*], Filip Janasz[1], Stephan Leyer[1]

[1] Faculty of Science, Technology and Medicine, Department of Engineering, University of Luxembourg, Luxembourg
[2] Faculty of Mechanical Engineering, Lodz University of Technology, Lodz, Poland

ARTICLE INFO

Article history:
Received 17 March 2025
Received in revised form 14 June 2025
Accepted 23 June 2025
Available online 15 July 2025

Keywords:
Multiphase flow; wire mesh sensor; bubble entrapment; CFD simulation; experimental validation; design optimization

ABSTRACT

Bubble entrapment in wire mesh sensors (WMS) reduces measurement accuracy in multiphase flows, posing a significant challenge for industrial applications. This study quantitatively evaluates the impact of wire diameters and spacing on bubble entrapment in WMS used for gas-liquid multiphase flow analysis. Combining experiments on low void fraction bubbly flow with computational fluid dynamics (CFD) simulations, the research investigates the dynamics of gas-liquid interfaces, focusing on how the sensor's geometric configuration affects capture efficiency. A 2D CFD simulation examined air bubbles with diameters of 3.5 mm, 5 mm, and 7 mm, and velocities from 0.054 m/s to 0.113 m/s in a circular vertical channel with 34 mm diameter. WMS design parameters analysed in this study included wire transverse pitch of 1 mm and 2 mm, and wire diameters of 0.2 mm and 0.125 mm, with a vertical pitch of 1.6 mm. Experimental tests used for validation investigated air bubbles with velocities from 0.25 m/s to 0.3 m/s in a channel of 34 mm in diameter. The findings reveal a complex interaction between WMS structural parameters and performance, identifying optimal design criteria that reduce bubble entrapment occurrences and thus improve the accuracy of flow measurements. Both CFD simulations and experiments demonstrated that bubbles are entrapped when surface tension forces between the wire, air, and water exceed the buoyancy forces of the bubbles, especially when wire spacing is small relative to bubble size.

1. Introduction

Wire mesh sensors (WMS) are an intrusive, tomographic tool to observe multiphase flow behavior at a channel's cross-section [1,2]. WMS can capture and resolve multiphase flow patterns by measuring the electrical conductivity and, more recently, capacitance with a grid of crisscrossing wires placed in a fluid. It applies only to two-phase flow where the two phases have significantly different electrical properties. Examples of such flows are water vapor or air bubbles in a vertical column of water [3,4]. The WMS applications are centered on gas-liquid flow measurement [5-9]. These sensors consist of two perpendicular planes of parallel wires. The transmitter wires emit electric pulses. A current, proportional to the fluid resistivity, flows to the receiver wires. It means

* *Corresponding author.*
E-mail address: iurii.dolganov@uni.lu

https://doi.org/10.37934/arfmts.133.2.2942

that if the cross-section point of the wire is momentarily surrounded by an electrically conductive fluid such as water the received pulse will have a high value. In contrast, when the crossing point of the wires is surrounded fluid which electric conductance can be approximated to be 0, the receiver will receive a low-value signal [10,11]. The crossing points are arranged in a square grid, Figure 1, and by combining the data from each, WMS can reconstruct detailed images of the phase distribution across the flow cross-section [12,13]. Figure 2 shows an example of a single bubble passing the 16 x 16 WMS.

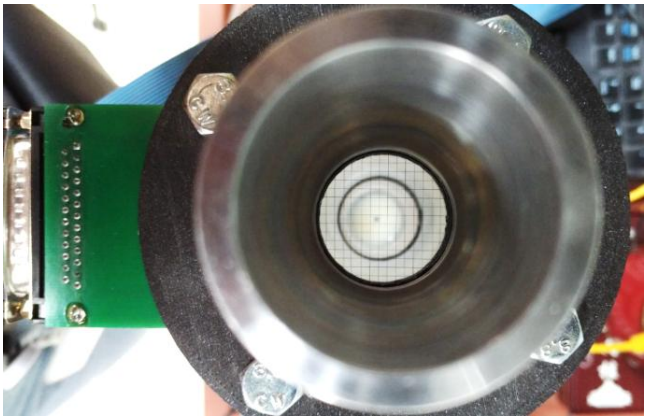

Fig. 1. Photo of the WMS installed in a vertical channel

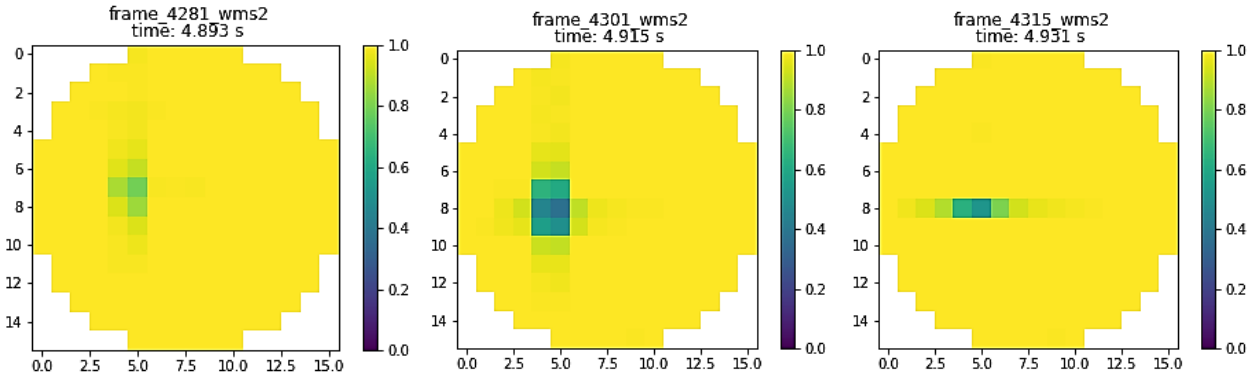

Fig. 2. The registered, unprocessed image of a single air bubble (blue cells) in water (yellow cells) as it passes through a 16 x 16 WMS

Bubble entrapment in WMS poses a significant challenge for accurate multiphase flow measurements in various industrial applications [3,14]. The issue of bubble entrapment often undermines the accuracy and reliability of the acquired data, particularly in flows with low void fractions. Recent advancements in sensor design have sought to address this issue by modifying the geometric and structural parameters of WMS, nonlinearity corrections, and improved electronic circuit design [12]. However, the complex interplay between these parameters and flow dynamics remains insufficiently explored. Most studies focus on operational principles and measurement techniques, leaving a gap in understanding how to optimize WMS design to minimize bubble entrapment. Therefore, the main objective of this paper is to study the interaction between structural parameters and WMS performance and to identify optimal design criteria that reduce the probability of bubble entrapment and thus improve the accuracy of flow measurements.

2. Methodology

Various numerical methods have been developed for the simulation of incompressible fluid flows, including the volume of fluid (VOF) method. Some alternative approaches, such as the vector form of interior finite element (VFIFE) method, have also been proposed to improve the analytical equilibrium in fluid modeling [15]. The methodology used in this study combines computational modeling in Ansys Fluent software and experimental validations to comprehensively analyze the performance of WMS. A 2D CFD model was developed using the volume of fluid (VOF) method to simulate the interaction between gas bubbles and sensor wires [16].

The selection of a two-dimensional CFD model was guided primarily by the need for computational cost for the case under study: wire diameters and spacings. Utilizing a 2D domain allowed extensive simulation coverage with adequate resolution while maintaining manageable computational time and resources. While the 2D approach provides valuable insight into the dominant physics of bubble-wire interactions, we acknowledge that it introduces several limitations:

i. Neglect of 3D flow structures, such as vortex shedding and bubble wobble or tilting, which may influence deformation and interaction with wire layers.
ii. Underestimation of curvature effects, especially in the vertical wire direction, which could slightly modify local pressure distribution around the bubble interface.
iii. Simplification of wire geometry, since actual wires form a 3D crisscross network rather than planar lines.

The model accounted for key parameters such as wire diameter, transverse pitch, bubble size, velocity, and liquid temperature. To validate the simulations, experiments were conducted in a controlled test facility, featuring a vertical glass channel equipped with WMS and a high-speed camera for capturing bubble dynamics. Air bubbles of various diameters were introduced at controlled velocities, and their interaction with the WMS was recorded. Key variables, including bubble velocity, entrapment rates, and deformation patterns, were measured and compared between simulations and experiments. This dual approach enabled cross-validation of results and provided a robust framework for assessing the impact of sensor design parameters. The methodology ensured that the findings were not only theoretically sound but also directly applicable to real-world scenarios, enhancing the reliability and industrial relevance of the study.

2.1. Geometry and CFD Simulation Parameters

The computational domain encompasses a vertical plane placed in a 34 mm diameter channel, at 45º to wire mesh sensor wires and as such is capable to capture both wire layers. The dimensions of the 2D model are presented in Figure 3. Different sensor configurations were modeled using wire diameters (0.125 mm and 0.2 mm) and spacing (1 mm and 2 mm). A detailed mesh, as shown in Figure 4, was developed and validated via a mesh independence study. The fluids used were defined as air and water, with properties adjusted to match the experimental conditions, such as density and viscosity at operational temperature. The inflow velocity was set as constant at the bottom of the channel while pressure-outlet conditions were applied at the top.

Subsequently, the k-ω turbulence model was used as it is suitable for low-Reynolds-number flows [17]. Three air bubbles of different diameters, 3 mm, 5 mm, and 7 mm, were introduced into the domain at the initialization stage with their centres placed 12.5 mm below the first layer of WMS wires. During the simulation, the bubbles would rise in the stagnant water due to the buoyancy forces. The VOF model was used to capture the interface between the air and water phases. Implicit volume fraction formulation and implicit body force are applied. Surface tension force modeling used

the continuum surface force model, and surface tension was adjusted to match experimental conditions using the real gas properties table data. Table 1 presents a summary of applied physics.

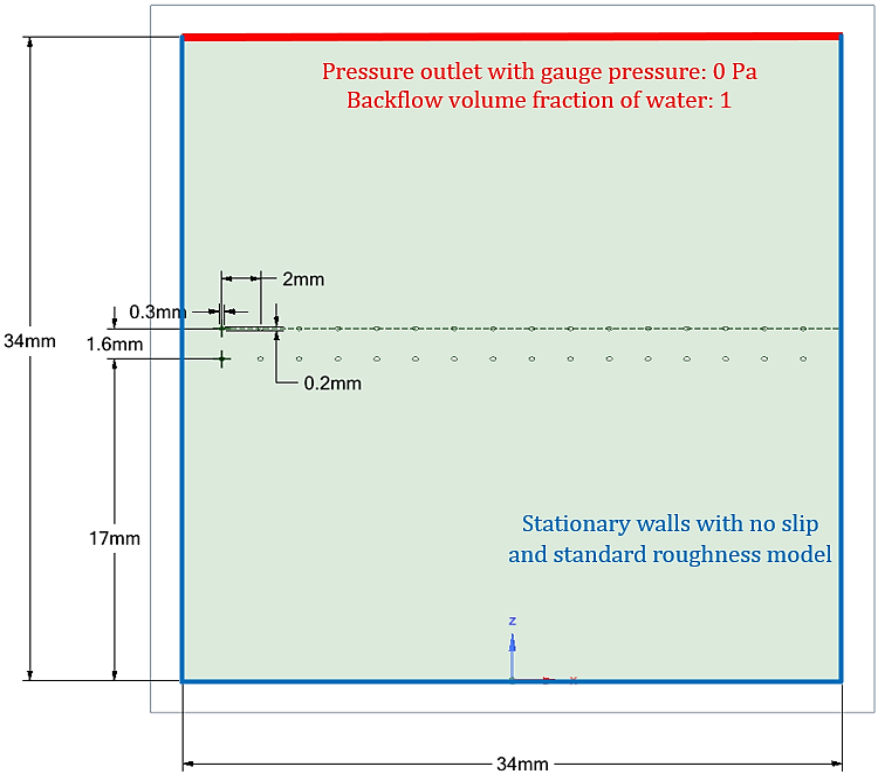

Fig. 3. Geometry used for simulation of WMS with 0.2 mm wire diameter and 2 mm transverse pitch

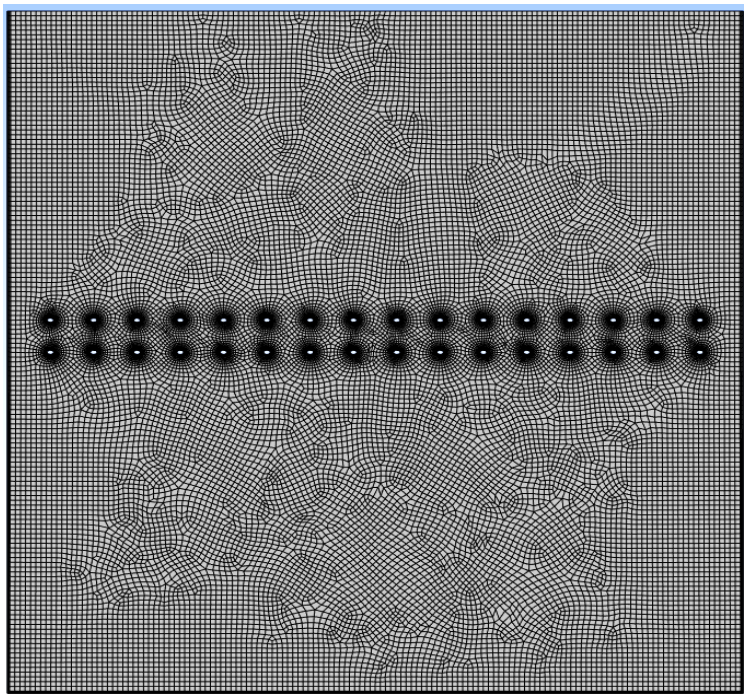

Fig. 4. Mesh used for simulation of WMS with 0.2 mm wire diameter and 2 mm transverse pitch

Table 1
Summary of the simulation parameters

General		
Solver	Type	Pressure-based
	Time	Transient
	Gravity	−9.81
Models		
Multiphase Model	Homogeneous model	Volume of fluid (VOF)
	Formulation	Explicit
		Courant number <2
	Lee evaporation-condensation	Improved by “real fluid” functions
Viscous model	k-ω	
Solution methods		
Pressure-velocity coupling	SIMPLE	
Spatial discretization	Pressure	PRESTO
	Volume fraction	Geo-reconstruct
	Momentum	First order upwind
Other settings		
Time step	Multiphase-specific adaptive with max. 0.0001875 s	

2.2 Experimental Validation

The validation of CFD results and the data obtained with WMS was carried out at the test facility at the University of Luxembourg (Figure 5). The installation was created considering the recommendations described in [18] and [19]. Data used for validation was obtained with a high-speed camera, synchronized to WMS DAS. The test facility (Figure 6) consists of a vertical glass tube 34 mm in diameter (1) with two wire mesh sensors spaced 92.5 mm from each other (2 and, 3) which are fixed in retaining flanges. The used WMS has a 0.2 mm wire diameter and a 2 mm transverse pitch. The data from the sensors are transmitted to the custom DAS (4). The tube with the sensors is rigidly fixed to the base (5). Air is supplied through the base via a capillary tube (6). The exact amount of the delivered air is regulated by a syringe pump (7). The temperature of the water in the cavity of the glass tube was measured using a temperature sensor (8). A high-speed video camera (10) is located perpendicular to the measuring section, and a reference ruler (9) is placed in the visual field, the data from which is transmitted directly to a DAS PC (11).

Fig. 5. Photo of the WMS test facility

For the correct operation of the sensors, the low and high reference signal amplitudes were calibrated in the complete absence of water and completely submerged conditions, respectively [20]. The water used for calibration and in the experiment had a defined electrical conductivity of 0.0421 µS/cm at 21.5 °C. Data from a high-speed video camera and WMS were used to determine the bubble's velocity using an algorithm developed by Prasser [21].

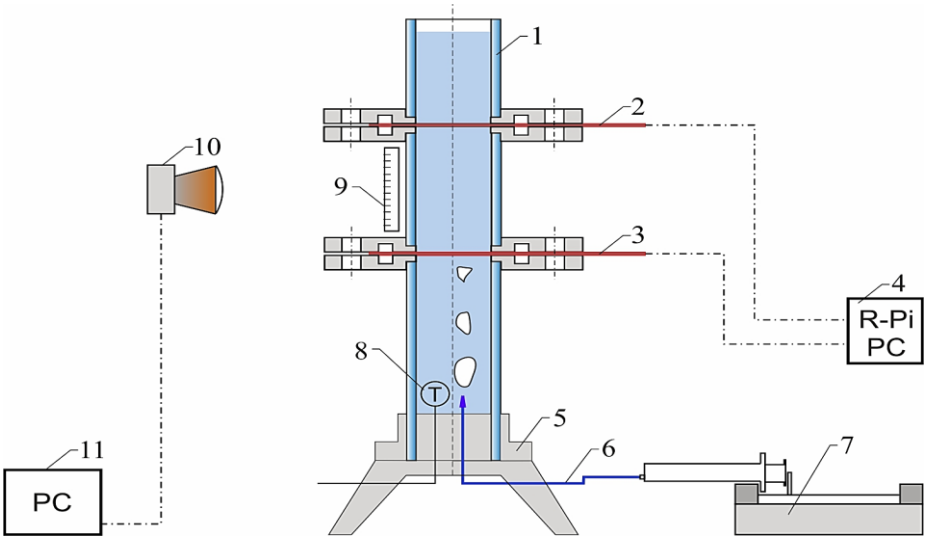

Fig. 6. Schematic view of the WMS calibration test facility. (1) Glass tube, (2, 3) wire-mesh sensor, (4) Raspberry Pi computer, (5) base holder, (6) air inlet (7) syringe pump, (8) temperature sensor, (9) measuring section with the ruler, (10) high-speed camera, and (11) laptop for HSC data collection

3. Results

3.1 CFD Results

The simulation results revealed a complex interaction between bubbles and sensors' wires, leading to several key insights into their design dependencies. Medium-sized bubbles were more likely to be entrapped by the bottom layer of the WMS due to insufficient buoyancy forces to overcome the surface tension forces at the interface between the sensor wires and the fluid phases. In contrast, the smallest bubbles, which were only slightly larger than the wire diameter, could easily pass through the mesh, often leading to an underestimation of their contribution to the overall void fraction in flow measurements. Additionally, as illustrated in Figure 7, WMS with larger diameter wires had a higher propensity to entrap bubbles compared to those with smaller diameter wires. This indicated that both wire diameter and spacing critically influenced the sensor's performance and accuracy.

The entrapped bubble, Figure 7, was observed to no longer be stuck on the layer of WMS when we introduced the following changes into the simulation:

i. Change of the water phase temperature to 40.7 °C (Figure 8(a)).
ii. Change of the water phase temperature to 61.2 °C (Figure 8(b)).
iii. Introduce water velocity at the bottom by using the bottom wall as an inlet (Figure 9).

One of the most crucial design parameters when designing a WMS for a specific application is wire spacing. Excessively small wire spacing leads to bubble entrapment due to surface tension forces, even for small wire diameters. This phenomenon significantly affects the accuracy of multiphase flow measurements.

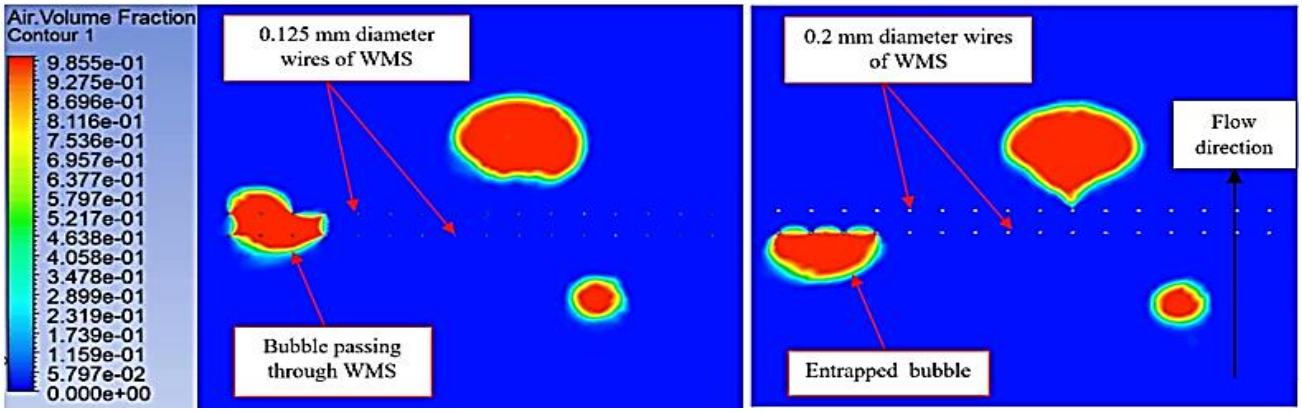

(a) (b)

Fig. 7. Simulation results (a) Air bubble passing through WMS with 0.125 mm wire diameter and 2 mm wire spacing (b) Air bubble entrapped on WMS with 0.2 wire diameter and 2 mm wire spacing

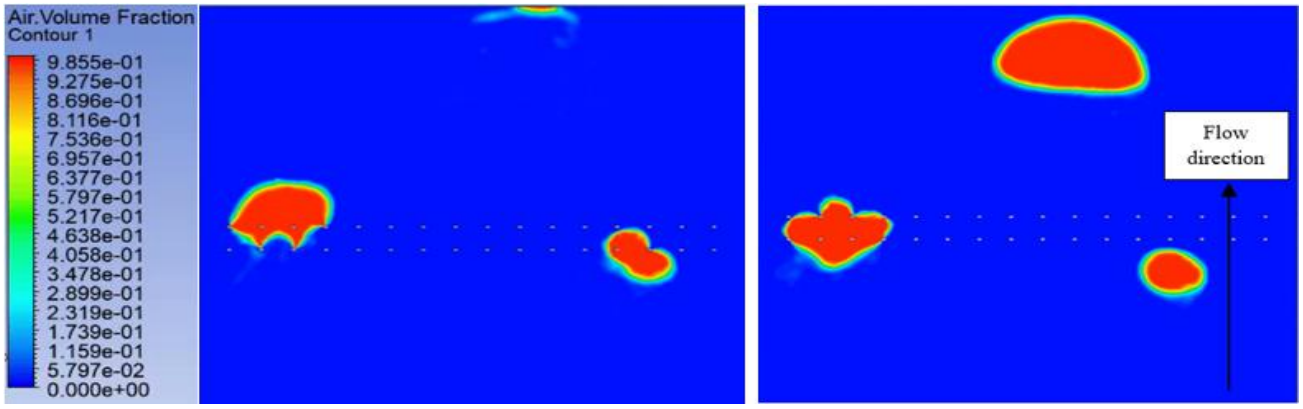

(a) (b)

Fig. 8. 5 mm bubble passing WMS with 0.2 mm wire diameter and 2 mm wire spacing due to increase in water temperature and thus decrease in surface tension. Water temperature (a) 40.7 °C (b) 61.2 °C

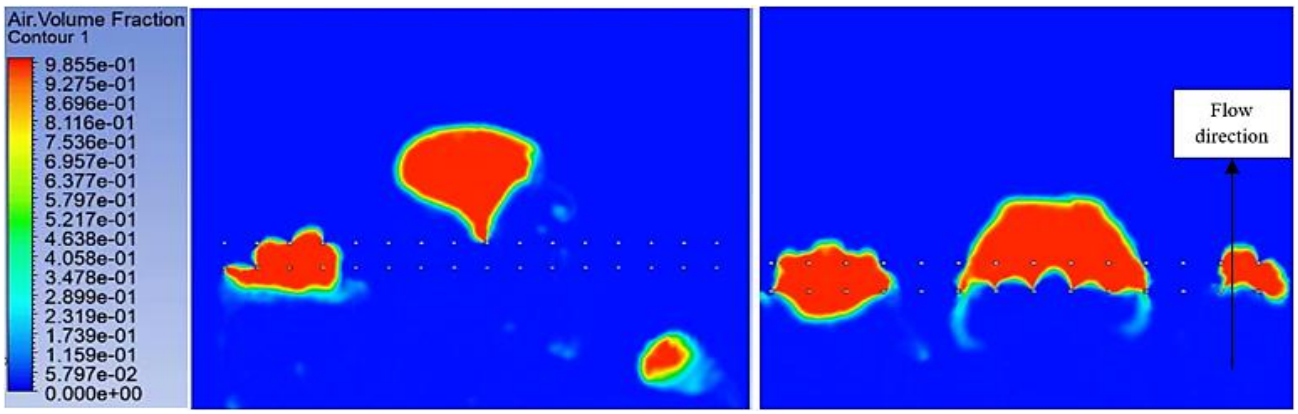

(a) (b)

Fig. 9. 5 mm bubble passing WMS with 0.2 mm wire diameter and 2 mm wire spacing due to the introduction of velocity water inlet on the bottom wall. Velocity inlet values (a) 0.02 m/s (b) 0.02 m/s

In analyzed cases (water temperature: 21.5 °C, 40.2 °C, and 61.2 °C), the mid-sized 5 mm bubble was not able to pass through the WMS under any conditions. When the water temperature was set to 40.2 °C, a 7 mm bubble passed through the sensor, but a 3.5 mm bubble was entrapped (Figure 10(a)). And when the water temperature was increased to 61.2 °C 7 mm and 3.5 mm passed through (Figure 10(b)). As expected, a smaller transverse pitch value (1 mm) demonstrated a high rate of

bubble capture. Conversely, a larger pitch (2 mm) facilitated easier bubble passage, although such a setup also could lead to the underestimation of potential smaller bubbles in the flow, which could pass through without detection by the sensors.

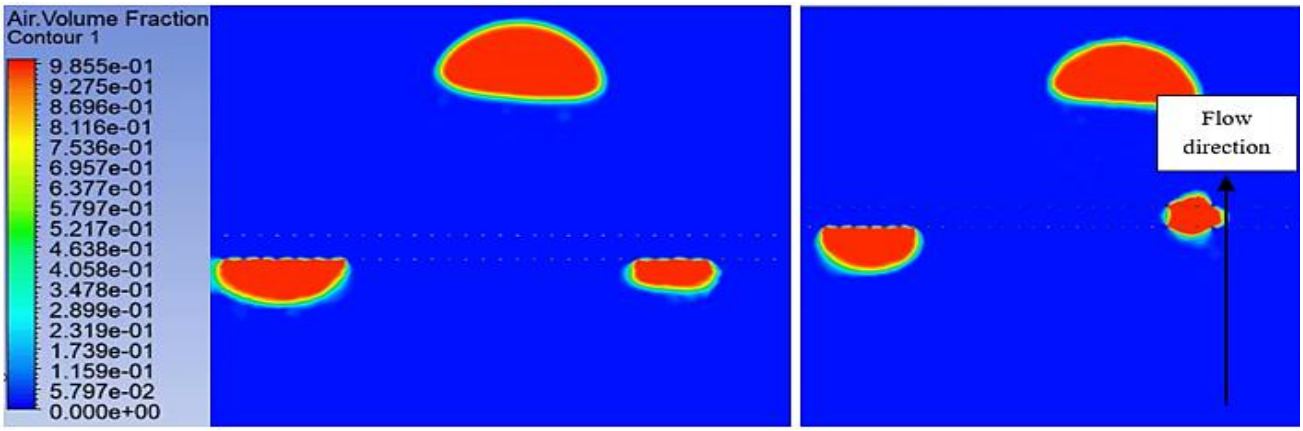

(a) (b)

Fig. 10. WMS with 1 mm pitch and 0.125 mm wire diameter (a) 7 mm bubble passing through in 40.2 °C water (b) 7 mm and 3.5 mm bubbles passing through in 61.2 °C water

3.2 Experimental Results

To validate the results of CFD modeling, a series of experiments were conducted with 0.2 mm wire diameter and 2 mm wire spacing WMS. For a temperature of 21.5 °C, bubbles with volumes of 0.05, 0.1, and 0.15 ml were entrapped in the sensor in most cases (Figure 11(a)). With an increase in temperature to 40.7 °C, the entrapment was limited to a bubble with a volume of 0.1 and 0.15 ml (Figure 11(b)). This observation aligns with the decrease of surface tension force at higher temperatures and points to these as a main factor in the entrapment.

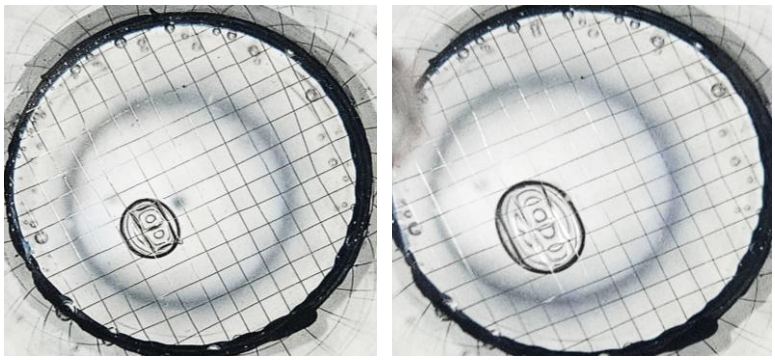

(a) (b)

Fig. 11. Air bubble entrapped on WMS (a) EXP I-2, V_{in} = 0,1 ml (b) EXP II-3, V_{in} = 0,15 ml

At 61.2 °C, no bubble entrapment was observed, which further confirms the surface tension effect. Increased injected air volume raised bubble velocity, while higher temperatures lowered surface tension. The sensor operated reliably with no bubble entrapment noted. The results of the series of experiments are collected in Table 2 and are in good agreement with the corresponding cases of the CFD model (Table 3). The entrapment occurs accordingly, and the difference in bubble velocities is explained by the fact that in the experiment, the initial impulse is given by a syringe pump, which somewhat overestimates the initial velocity in the experiment. It is important to note

the assumption that during the experiment, only the volume of air injected by the syringe pump was measured, and geometric dependencies determined the corresponding bubble diameter.

Table 2
Experimental results

	EXP	Temperature	Surface tension	Air injection	Approximate bubble diameter	Velocity	Bubble behavior
№	№	T, °C	σ, N/m	V_{in}, ml	D_b, mm	υ, m/s	-
I	1	21.5	0.0729	0.05	4.57	0.2585	Entrapped
	2			0.1	5.76	0.2608	Entrapped
	3			0.15	6.59	0.3045	Entrapped
	4			0.2	7.26	0.2877	Passing
	5			0.25	7.82	0.2971	Passing
II	1	40.7	0.0696	0.05	4.57	0.2704	Passing
	2			0.1	5.76	0.2571	Entrapped
	3			0.15	6.59	0.2789	Entrapped
	4			0.2	7.26	0.2787	Passing
	5			0.25	7.82	0.2948	Passing
III	1	61.2	0.066	0.05	4.57	0.2525	Passing
	2			0.1	5.76	0.2685	Passing
	3			0.15	6.59	0.2572	Passing
	4			0.2	7.26	0.2833	Passing
	5			0.25	7.82	0.3003	Passing

3.3 WMS Impact on Bubble Velocity and Shape

The intrusive nature of the WMS not only led to bubble entrapment but also slowed down the passing bubbles. As shown in Table 3, the difference in velocity reduction of the examined bubble at room temperature between the larger wire diameter (0.2 mm) WMS and the smaller wire diameter (0.125 mm) WMS differs significantly for different sizes of bubbles. The bubble velocity presented in Table 3 was derived from data captured over a distance of 17 mm, starting from 5 mm before the first layer of wires in the sensor. While bubble velocity data is reported, it should be noted that in the experimental setup, this parameter is subject to variability due to initial injection dynamics. Despite using a high-precision syringe pump, air compressibility and impulse effects introduce transient velocity spikes that are difficult to quantify reliably. Consequently, velocity was treated as a qualitative indicator rather than a quantitative validation metric for simulation results.

7 mm diameter bubble was 45% slower while passing through a 0.2 mm wire diameter, 2 mm pitch WMS in comparison to the setup with 0.125 mm wire diameter. On the other hand, the 3.5 mm bubble was slowed down by only 19% by a wire-mesh sensor with a bigger wire diameter. Moreover, it was observed that the increase in the water temperature decreased the slowdown of the bubbles. 7 mm diameter bubble passing through 2 mm pitch WMS was moving approximately 47% faster in water temperature of 61.2 °C as compared against 21.5°C. The observed bubble slowdown in the examined cases, as they contact the wire mesh sensor, aligns with findings from previous research [7]. According to the cited study, this slowdown is attributed to the decelerating forces that occur when the gas-liquid interface interacts with the solid surface of the wire mesh sensor.

The simulations further revealed that bubbles tended to flatten as they traversed through a wire mesh sensor, undergoing temporary deformation. However, they largely reverted to their original shape after passing through the sensor, as depicted in Figure 12. Notably, the degree of flattening varied with bubble size and velocity; larger bubbles and higher velocities resulted in more pronounced deformation. This transient shape change highlighted the dynamic interaction between

the bubbles and the sensor structure, emphasizing the importance of accounting for these effects to ensure accurate measurement and analysis of multiphase flows. The change of bubble shape has also been observed in high-speed camera data.

Table 3
Simulation-based estimation of bubble velocities passing through WMS

Temperature, °C	Bubble diameter, mm	Wire diameter, mm	Wire spacing, mm	Bubble velocity, m/s
21.5	7	0.2	2	0.0547
		0.125	2	0.0995
		0.125	1	Entrapped
	5	0.2	2	Entrapped
		0.125	2	0.0619
		0.125	1	Entrapped
	3.5	0.2	2	0.0880
		0.125	2	0.109
		0.125	1	Entrapped
40.7	7	0.2	2	0.1035
		0.125	1	0.0921
	5	0.2	2	0.0892
		0.125	1	Entrapped
	3.5	0.2	2	0.0881
		0.125	1	Entrapped
61.2	7	0,2	2	0.1039
		0.125	1	0.07957
	5	0.2	2	0.0895
		0.125	1	Entrapped
	3.5	0.2	2	0.0765
		0.125	1	0.1132

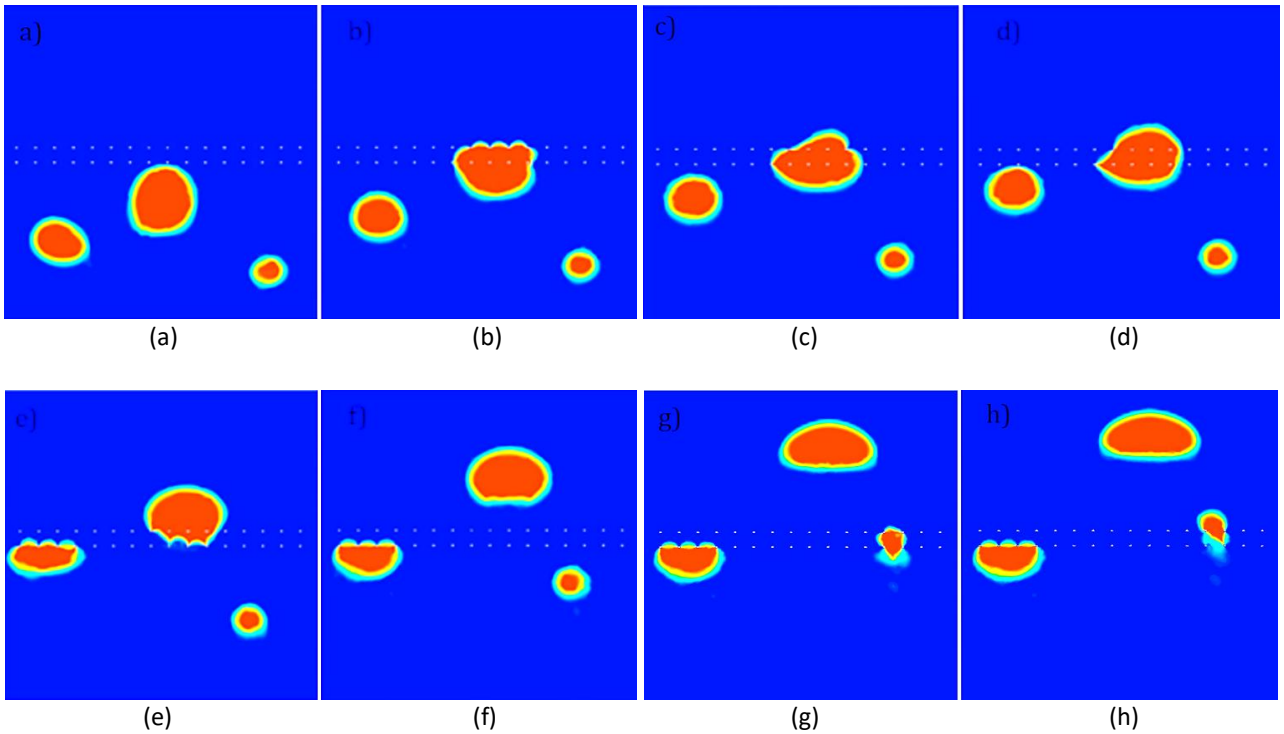

Fig. 12. Simulation of bubble behavior as it is passing through the wire mesh sensor at 21.5 °C. Time values, s (a) 0.366 (b) 0.450 (c) 0.477 (d) 0.489 (e) 0.523 (f) 0.578 (g) 0.618 (h) 0.631. Scale bar and flow direction are the same as on Figures 7 to 10

3.4 Optimization of Wire Mesh Sensor Design

The optimization of WMS design requires balancing several key parameters, such as wire diameter, wire spacing, and the operational conditions (temperature, bubble size, velocity). The goal is to minimize bubble entrapment while maintaining high measurement accuracy. This section presents an analytical approach to determine the optimal wire thickness based on fluid properties, bubble dimensions, and temperature effects.

3.4.1 Surface tension and buoyancy force

Bubble entrapment occurs when the surface tension force (F_s) between the wire and air/water interface exceeds the buoyancy force (F_b) of the bubble. These forces can be expressed as follows:

$$F_s = \sigma L \cos\theta F_b = \rho_g V_b g \tag{1}$$

where σ is the surface tension coefficient of water (temperature-dependent), L is the wetted perimeter of the wire, θ is the contact angle, ρ_g is the density of gas (air), V_b is the bubble volume, and g is the gravitational acceleration. For optimal design, we require that $F_b > F_s$, ensuring that bubbles can escape rather than being trapped. Validation calculation**:** Using experimental data from Table 2, for a 5.76 mm bubble at 21.5°C:

$$F_b = 1.225 \cdot 1.005 \cdot 10^{-6} \cdot 9.81 = 1.206 \cdot 10^{-5} N \tag{2}$$

$$F_s = 0.0729 \cdot 0.2\pi \cos(80°) = 2.67 \cdot 10^{-5} N \tag{3}$$

Since $F_b < F_s$, the bubble is likely to be trapped, which matches the experimental results.

3.4.2 Optimal wire thickness determination

Using experimental and simulation data, we derive an empirical relationship for the optimal wire diameter d_w that prevents entrapment as follows:

$$d_w \leq {}^{2\sigma}/_{\rho_g g D_b} \tag{4}$$

where D_b is bubble diameter. For a 5 mm bubble at 21.5°C:

$$d_w \leq {}^{2 \cdot 0.0729}/_{1.225 \cdot 9.81 \cdot 0.005} = 24 \text{ mm} \tag{5}$$

This suggests that the 0.2 mm wire used in experiments may have contributed to bubble entrapment, and a thinner wire (e.g., 0.125 mm) would be preferable. Subsequently, all the experimental results were analyzed using the obtained formula and summarized in Table 4. In all cases, the calculated surface tension force is greater than the buoyancy force, meaning bubbles are likely to be trapped, aligning with experimental observations. The values listed under "optimal wire diameter" are theoretical estimates based on the balance of surface tension and buoyancy forces. They are intended to define upper bounds and trends in design optimization, rather than represent practical wire sizes for experimental implementation. Based on the data in Table 5, we propose the following

practical threshold for avoiding bubble entrapment in wire mesh sensors. It is generally sufficient to allow bubble passage. These empirical ratios serve as a quick evaluation when designing or selecting wire configurations for given operating conditions.

Table 4
Optimal wire diameter based on experimental analysis

Bubble millimetre, mm	Temperature, °C	Surface tension, N/m	Bubble volume, m^3	Wire diameter used, mm	Buoyancy force, N	Surface tension force, N	Bubble trapped?	Optimal wire diameter, mm
3.2	21.5	0.0729	1.7×10^{-7}	0.125	0.000002	0.007954	Yes	3.79
4.5	40.7	0.0696	4.7×10^{-7}	0.125	0.000006	0.007594	Yes	2.57
5.76	61.2	0.0660	1.0×10^{-6}	0.2	0.000012	0.007201	Yes	1.91
6.9	21.5	0.0729	1.7×10^{-6}	0.2	0.000020	0.007954	Yes	1.76
7.8	40.7	0.0696	2.5×10^{-6}	0.25	0.000030	0.007594	Yes	1.49

Table 5
Practical threshold for avoiding bubble entrapment

Bubble diameter, mm	Temperature, °C	Recommended max wire diameter d_w [mm]	Ratio D_b/d_w
3.5	21.5	≤ 0.12	≥ 29
5.0	40.7	≤ 0.2	≥ 25
7.0	61.2	≤ 0.35	≥ 20

4. Conclusion

This study has demonstrated that the design parameters of WMS, specifically wire diameter and spacing, significantly impact bubble entrapment phenomena in multiphase flows. Through a combination of CFD simulations, it was found that smaller wire spacings relative to bubble size and larger wire diameters increase the likelihood of bubble entrapment due to surface tension forces. Conversely, appropriately sized wires and spacings allow bubbles to pass through the sensor, enhancing measurement accuracy. These findings suggest that optimizing wire diameter and spacing can reduce bubble entrapment, thereby improving the accuracy of WMS in multiphase flow analysis. To sum up, during both experiments and simulations, it was observed that:

i. Wire mesh sensors (WMS) with larger transverse pitches and wire diameters are more susceptible to bubble entrapment at room temperature.
ii. Wires with larger diameters are generally more prone to bubble entrapment compared to those with smaller diameters.
iii. Smaller transverse pitches can enhance the spatial resolution of wire mesh sensors but may also increase the likelihood of bubble entrapment.
iv. Larger transverse pitches tend to reduce the risk of bubble entrapment but may compromise spatial resolution.
v. The increase in water temperature decreases the chance of bubbles getting trapped in the WMS as water-air surface tension decreases with the increase in temperature.
vi. Low-velocity bubbles are more prone to being entrapped within the wire mesh sensor but less prone to being cut and fragmented by the wires.
vii. WMS can entrap the bubble on a single layer of bubbles when the bubble has very low energy, as we learned from simulation results, or can entrap it between the two layers of bubbles, as proven during the experiment.

Based on the derived equations and experimental validation, the following recommendations are proposed:

i. For small bubbles (3-5 mm), use thin wires (0.125 mm) with larger spacing (2 mm) to allow easier passage.
ii. For larger bubbles (7 mm and above), a wire diameter of 0.2 mm can be used, but adjustments in pitch spacing are required to reduce entrapment risk.
iii. For high-temperature applications (> 40°C), a reduction in wire diameter is necessary due to lower surface tension effects.

Future research should further explore design parameters such as vertical pitch, transverse pitch, and wire diameter using both 2D and 3D CFD simulations, along with experimental setups. Additionally, it is crucial to investigate WMS intrusiveness under a wider range of working conditions, including varying bubble sizes, broader temperature ranges, different types of fluids, and liquid velocities. This will help extend the applicability of WMS to diverse industrial settings, ensuring accurate and reliable multiphase flow measurements.

Acknowledgment
This research was not funded by any grant

References

[1] Prasser, H-M., Arnd Böttger, and Jochen Zschau. "A new electrode-mesh tomograph for gas–liquid flows." *Flow Measurement and Instrumentation* 9, no. 2 (1998): 111-119. https://doi.org/10.1016/S0955-5986(98)00015-6
[2] Prasser, H-M., Danilo Scholz, and Cornelius Zippe. "Bubble size measurement using wire-mesh sensors." *Flow Measurement and Instrumentation* 12, no. 4 (2001): 299-312. https://doi.org/10.1016/S0955-5986(00)00046-7
[3] Zaruba, Alexandr, Eckhard Krepper, H-M. Prasser, and BN Reddy Vanga. "Experimental study on bubble motion in a rectangular bubble column using high-speed video observations." *Flow Measurement and Instrumentation* 16, no. 5 (2005): 277-287. https://doi.org/10.1016/j.flowmeasinst.2005.03.009
[4] Perez, V. Hernandez, B. J. Azzopardi, R. Kaji, M. J. Da Silva, M. Beyer, and U. Hampel. "Wisp-like structures in vertical gas–liquid pipe flow revealed by wire mesh sensor studies." *International Journal of Multiphase Flow* 36, no. 11-12 (2010): 908-915. https://doi.org/10.1016/j.ijmultiphaseflow.2010.08.002
[5] Peña, HF Velasco, and O. M. H. Rodriguez. "Applications of wire-mesh sensors in multiphase flows." *Flow Measurement and Instrumentation* 45 (2015): 255-273. https://doi.org/10.1016/j.flowmeasinst.2015.06.024
[6] Richter, S., M. Aritomi, H-M. Prasser, and R. Hampel. "Approach towards spatial phase reconstruction in transient bubbly flow using a wire-mesh sensor." *International Journal of Heat and Mass Transfer* 45, no. 5 (2002): 1063-1075. https://doi.org/10.1016/S0017-9310(01)00211-3
[7] Hampel, U., J. Otahal, S. Boden, M. Beyer, E. Schleicher, W. Zimmermann, and M. Jicha. "Miniature conductivity wire-mesh sensor for gas-liquid two-phase flow measurement." *Flow Measurement and Instrumentation* 20, no. 1 (2009): 15-21. https://doi.org/10.1016/j.flowmeasinst.2008.09.001
[8] Pietruske, Heiko, and Horst-Michael Prasser. "Wire-mesh sensors for high-resolving two-phase flow studies at high pressures and temperatures." *Flow Measurement and Instrumentation* 18, no. 2 (2007): 87-94. https://doi.org/10.1016/j.flowmeasinst.2007.01.004
[9] Da Silva, M. J., S. Thiele, L. Abdulkareem, B. J. Azzopardi, and U. Hampel. "High-resolution gas–oil two-phase flow visualization with a capacitance wire-mesh sensor." *Flow Measurement and Instrumentation* 21, no. 3 (2010): 191-197. https://doi.org/10.1016/j.flowmeasinst.2009.12.003
[10] Prasser, Horst-Michael, Matthias Beyer, Thomas Frank, Suleiman Al Issa, Helmar Carl, Heiko Pietruske, and Peter Schütz. "Gas–liquid flow around an obstacle in a vertical pipe." *Nuclear Engineering and Design* 238, no. 7 (2008): 1802-1819. https://doi.org/10.1016/j.nucengdes.2007.11.007
[11] Omebere-Iyari, N. K., B. J. Azzopardi, D. Lucas, M. Beyer, and H. M. Prasser. "The characteristics of gas/liquid flow in large risers at high pressures." *International Journal of Multiphase Flow* 34, no. 5 (2008): 461-476. https://doi.org/10.1016/j.ijmultiphaseflow.2007.11.001
[12] de Assis Dias, Felipe, Philipp Wiedemann, Eckhard Schleicher, Marco Jose da Silva, and Uwe Hampel. "Improvement of wire-mesh sensor accuracy via adapted circuit design and integrated energy loss measurement." *Measurement Science and Technology* 33, no. 8 (2022): 084002. https://doi.org/10.1088/1361-6501/ac6ab4

[13] Da Silva, M. J., E. Schleicher, and U. Hampel. "Capacitance wire-mesh sensor for fast measurement of phase fraction distributions." *Measurement Science and Technology* 18, no. 7 (2007): 2245. https://doi.org/10.1088/0957-0233/18/7/059
[14] Xiong, Jinbiao, Hao Xie, Sijia Du, and Xu Cheng. "Experimental measurement of bubbly two-phase flow in a 4x4 rod bundle with wire mesh sensor." *Applied Thermal Engineering* 218 (2023): 119294. https://doi.org/10.1016/j.applthermaleng.2022.119294
[15] Samy, Akram, Shu Li, Xingfei Yuan, Chengwei Liu, and Yongcan Dong. "Vector form of intrinsic finite element method for incompressible fluids." *Computers & Fluids* 279 (2024): 106319. https://doi.org/10.1016/j.compfluid.2024.106319
[16] Parsi, M., R. E. Vieira, M. Agrawal, V. Srinivasan, B. S. Mclaury, S. A. Shirazi, E. Schleicher, and U. Hampel. "Computational fluid dynamics (CFD) simulation of multiphase flow and validating using wire mesh sensor." In *BHR International Conference on Multiphase Production Technology*, p. BHR-2015. BHR, 2015.
[17] Aftab, S. M. A., A. S. Mohd Rafie, N. A. Razak, and K. A. Ahmad. "Turbulence model selection for low Reynolds number flows." *PloS one* 11, no. 4 (2016): e0153755. https://doi.org/10.1371/journal.pone.0153755
[18] Tompkins, Casey, Horst-Michael Prasser, and Michael Corradini. "Wire-mesh sensors: A review of methods and uncertainty in multiphase flows relative to other measurement techniques." *Nuclear Engineering and Design* 337 (2018): 205-220. https://doi.org/10.1016/j.nucengdes.2018.06.005
[19] Prasser, Horst-Michael, and Richard Häfeli. "Signal response of wire-mesh sensors to an idealized bubbly flow." *Nuclear Engineering and Design* 336 (2018): 3-14. https://doi.org/10.1016/j.nucengdes.2017.04.016
[20] Schubert, Markus, Holger Kryk, and Uwe Hampel. "Slow-mode gas/liquid-induced periodic hydrodynamics in trickling packed beds derived from direct measurement of cross-sectional distributed local capacitances." *Chemical Engineering and Processing: Process Intensification* 49, no. 10 (2010): 1107-1121. https://doi.org/10.1016/j.cep.2010.08.004
[21] Prasser, Horst-Michael, and Matthias Beyer. "Bubble recognition algorithms for the processing of wire-mesh sensor data." In *Proceedings of 6th International Conference on Multiphase Flow* 719, p. 1-9. 2007.